

The Process of Electrooxidation of Quercetin 3,4'-di-*O*- β -Glucopyranoside at Glassy Carbon Electrode

Boguslaw Pierozynski and Danuta Zielinska*

Department of Chemistry, Faculty of Environmental Management and Agriculture,
University of Warmia and Mazury in Olsztyn, Plac Lodzki 4, 10-727 Olsztyn, Poland

RECEIVED MAY 14, 2009; REVISED AUGUST 10, 2009; ACCEPTED SEPTEMBER 9, 2009

Abstract. The present paper reports electrochemical and UV-VIS spectroscopic studies on the process of electrooxidation of quercetin 3,4'-di-*O*- β -glucopyranoside (Q 3,4'-diglc) molecule, at glassy carbon electrode surface in 0.1 M sodium acetate – acetic acid buffer in 90 % methanol solution. The process starts at 3'-OH group (ring B), followed by oxidation of 5,7-dihydroxyl group in ring A. As a result of electrochemical reactions, the surface area of glassy carbon (GC) electrode becomes extensively blocked by Q 3,4'-diglc oxidation products.

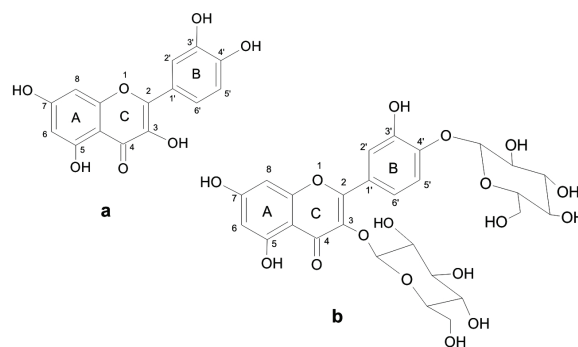
Keywords: Q 3,4'-diglc electrooxidation, cyclic voltammetry, impedance spectroscopy, UV-VIS spectroscopy

INTRODUCTION

Flavonoids are widely distributed plant secondary metabolites. They have significant impact on essential growth of plants, simultaneously protecting them against various biotic and abiotic stresses.¹ As a part of human diet, flavonoids are responsible for preventing various degenerative diseases.² These polyphenolic compounds are characterized by two aromatic cycles (rings A and B) that are linked by a heterocycle (ring C). Flavonoids are known to undergo oxidation or reduction electron transfer reactions. In general, the electrochemical reactivity of hydroxyflavones decreases in a sequence: catechol OH group (ring B), 2,3-double bond in conjunction with 4-oxo group and 3-hydroxyl group (ring C), following 5,7-dihydroxyl group (ring A).³ As a consequence, the antioxidant activity of flavonoids is primarily determined by the most reactive sites, *i.e.* those associated with rings B and C. On the other hand, the activity of the 5,7-dihydroxyl group is rather insignificant.⁴⁻⁶ The electrochemical behaviour of flavonoids, such as: rutin, quercetin and catechin has extensively been studied in works by Hendrickson *et al.*⁷ and Timbola *et al.*,⁸ by Zhou *et al.*⁹ and Zare *et al.*,¹⁰ and by Martinez *et al.*¹¹ and Janeiro, and Brett,¹² correspondingly.

In plants, flavonoids mostly exist as various *O*- β -glucosides, with mainly D-glucose as a sugar residue. For example, quercetin in tea, onions and apples occurs in four major forms, as: quercetin aglycone (Scheme 1,

compound a), quercetin-3,4'-di-*O*- β -glucoside (Scheme 1, compound b), quercetin-3-*O*- β -glucoside and quercetin-4'-*O*- β -glucoside.^{6,13,14} Quercetin glucosides represent dietary constituents of paramount importance. For example, about 99 % of quercetin in shallot flesh is formed by its glucosides, mainly by quercetin-3,4'-di-*O*- β -glucoside and to a much smaller extent by quercetin-4'-*O*- β -glucoside.² Antioxidant properties of quercetin glucosides are strongly dependent on their chemical structure and can conveniently be studied by a combination of electrochemical and spectroscopy methods. The main aim of this work was to investigate the electrochemical behaviour of quercetin-3,4'-di-*O*- β -glucopyranoside (see Scheme 1, compound b) at glassy carbon electrode,



Scheme 1. (a) Chemical structure of: 3,3',4',5,7-pentahydroxyflavone (quercetin, Q), (b) quercetin 3,4'-di-*O*- β -glucopyranoside (Q 3,4'-diglc).

* Author to whom correspondence should be addressed. (E-mail: dziei@uwm.edu.pl)

with special consideration of the mechanism and the kinetics of the Q 3,4'-diglc electrooxidation process.

EXPERIMENTAL

Solutions and Chemical Reagents

All solutions were prepared from analytical grade chemicals, including: methanol, sodium acetate and acetic acid (Polish Chemical Compounds, POCH, Poland), and Q 3,4'-diglc (Polyphenol Laboratories SA, Norway). A stock solution of Q 3,4'-diglc in methanol was prepared and the concentration of Q 3,4'-diglc in the solution was verified by the UV spectroscopy measurements.¹⁵ In addition, high quality water of 18.2 MΩ cm resistivity was supplied by a Direct-Q3 UV ultra-pure water purification system from Millipore. A supporting electrolyte was 0.1 M sodium acetate-acetic acid buffer in 90 % CH₃OH, and Q 3,4'-diglc concentration was 0.25×10^{-3} M. The experiments were carried-out at pH = 5.0 and 7.5.

Equipment and Experimental Methodology

An electrochemical cell made all of Teflon was used during the course of this work. The cell (with a total volume of 0.2 mL) comprised three electrodes: a glassy carbon (GC) working electrode (BAS MF-2012, 3 mm diameter), an Ag|AgCl (3.5 M KCl) reference (RE) and a Pt (0.5 mm diameter coiled Pt wire) counter electrode (CE). Prior to each experiment, the cell was taken apart, rinsed with Millipore ultra-pure water and methanol. The GC working electrode was carefully hand-polished before each experiment with 0.05 μm alumina-water paste (BAS CF-1050), using BAS (MF-1040) polishing cloth. Then, the electrode was thoroughly rinsed with ultra-pure water and finally with methanol.

All a.c. impedance and cyclic voltammetry measurements were conducted at room temperature by means of the Solartron 12608W Full Electrochemical System, consisting of 1260 frequency response analyzer (FRA) and 1287 electrochemical interface (EI). For impedance measurements, the generator provided an output signal of known amplitude (5 mV) and the frequency range was typically swept between 1.0×10^5 and 5.0×10^{-2} Hz. The instruments were controlled by ZPLOT 2.9 or CORWARE 2.9 software for Windows (Scribner Associates, Inc.). Presented here results were obtained through analysis of representative series of experimental data (3–5 impedance measurements were usually carried-out at each potential value). Data analysis was performed with ZVIEW 2.9 or CORRVIEW 2.9 software package, where the impedance spectra were fitted by means of a complex, non-linear, least-squares imittance fitting program, LEVM 6 (written by J. R. Macdonald, Ref. 16).

UV-visible Spectral Analysis

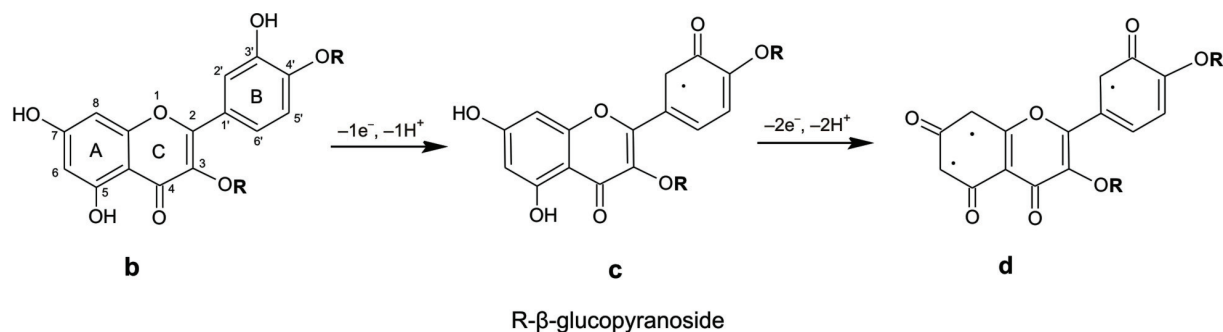
In order to allow identification of Q 3,4'-diglc electro-oxidation products, UV-visible spectral analysis was conducted on pre-electrolyzed (at the constant potential of 1.000 mV) 50 μM base solution at pH = 7.5. The progress of electrolysis was controlled by recording the spectra after: 30, 60, 120 and 180 minutes following electrolysis start up. The process of electrolysis was carried-out in a simple, beaker-type (20 mL) cell, where a large surface-area (ca. 300 cm²) carbon fibre electrode (Hexcel 12K AS4C) was used as a working electrode. An UV-160 IPC spectrophotometer, with CPS Controller (Shimadzu, Japan) was employed to perform UV-visible spectrophotometric measurements.

RESULTS AND DISCUSSION

Electrooxidation of Q 3,4'-diglc at GC Electrode by Cyclic Voltammetry

To date, little information on the electrochemical properties of flavonoid glycosides can be found in available literature.^{8,13,17} The process of electrochemical oxidation of quercetin glycosides at GC electrode is not fully understood. However, it is generally accepted that the reaction proceeds through a cascade mechanism, which initially leads to oxidation of catechol OH group in ring B, followed by oxidation of the remaining hydroxyl groups in rings C and A.¹⁷ The oxidation process of quercetin glycosides is strongly pH dependent.¹⁸ At pH values above ca. 7.0, deprotonation of the hydroxyl groups becomes facilitated, which does significantly affect the process of electron donation.^{7,9,10,13} For the purpose of this work, we studied the electrochemical behaviour of Q 3,4'-diglc in slightly acidic solution (pH = 5.0) and in electrolyte of nearly physiological pH of 7.5.

The cyclic voltammetric behaviour of Q 3,4'-diglc at the GC electrode in 0.1 M acetate-acetic buffer solution (at pH = 5.0 and 7.5) is shown in Figures 1a and b, respectively. It can be seen in these Figures that position of the centre of the first oxidation peak (denoted as peak 1 in Figures 1a and 1b) is shifted negatively from 800 mV at pH = 5.0 (Figure 1a) to 680 mV at pH = 7.5 (Figure 1b). An additional oxidation peak is observed at ca. 1.050 mV, but unambiguously only for pH = 5.0 (see peak 2 in Figure 1a). The two voltammetric peaks (peak 1 and peak 2) observed in Figure 1a are the result of irreversible oxidation processes that are concerned with the 3'-OH group in ring B (peak 1 centred at 800 mV) and the 5,7-dihydroxyl group of ring A (peak 2 centred at ca. 1.050 mV). Consequently, no reduction peaks were observed upon reversal of the voltammetric sweep (see Figures 1a and 1b again). Schematic diagrams of proposed electrooxidation steps for Q 3,4'-diglc (with respect to peak 1 and peak 2 in Figures 1a and 1b)



Scheme 2. Proposed, schematic diagram of an initial electrooxidation step for Q 3,4'-diglc molecule, at glassy carbon electrode surface, compound c, for the following oxidation step (involving 5,7-dihydroxyl group on ring A), compound d.

are shown in Scheme 2. An initial electrooxidation step is a one-electron, one-proton charge-transfer reaction, (Scheme 2, compound c) while the consecutive step involves a two-electron, two-proton irreversible charge-transfer reaction (Scheme 2, compound d).

Strong adsorption of Q 3,4'-diglc oxidation product(s) on the GC surface leads to severe surface poisoning (compare the successive voltammetric scans 1 through 5 in Figures 1a and b), which effect is much more pronounced at pH = 7.5, as compared to that observed at pH = 5.0. Similar findings were observed in work by Castaignede *et al.*¹⁹

UV-visible Spectra Analysis of Electrolyzed Q 3,4'-diglc-Based Buffer Solution

Figure 2a shows the UV-visible spectra, recorded before and during the constant potential (conducted at 1.000 mV vs. Ag|AgCl) electrolysis. Two maxima are initially observed in Figure 2a; first centred at 348.4 nm (band I) and another one localized at *ca.* 260 nm (band II). The first maximum corresponds to the conjunction between rings B and C, while the second maximum (band II) refers to the ring A portion of the Q 3,4'-diglc molecule. A significant band splitting that is observed for band II in Figure 2a ($\lambda_1 = 253.6$ nm and $\lambda_2 = 265.6$ nm) can possibly be the effect of mutual interaction between the glucopyranoside functional group and the 5,7-dihydroxyl group on ring A (see again Scheme 1).²⁰ A continuous intensity reduction for both bands in Figure 2a is observed during the course of electrolysis. The above can be explained in terms of progressive electrooxidation process (see again Scheme 2) that takes place on the GC surface. Consequently, the products of electrolysis become partly stripped off from the electrode and undergo dissolution in the supporting electrolyte. Figure 2b below shows a continuous effect of the Q 3,4'-diglc surface electrooxidation process on the GC electrode. It can be seen in this Figure that peak 1 (characteristic of the 3'-OH group oxidation) has almost disappeared from the CV profile after 3 hours of potentiostatic electrolysis.

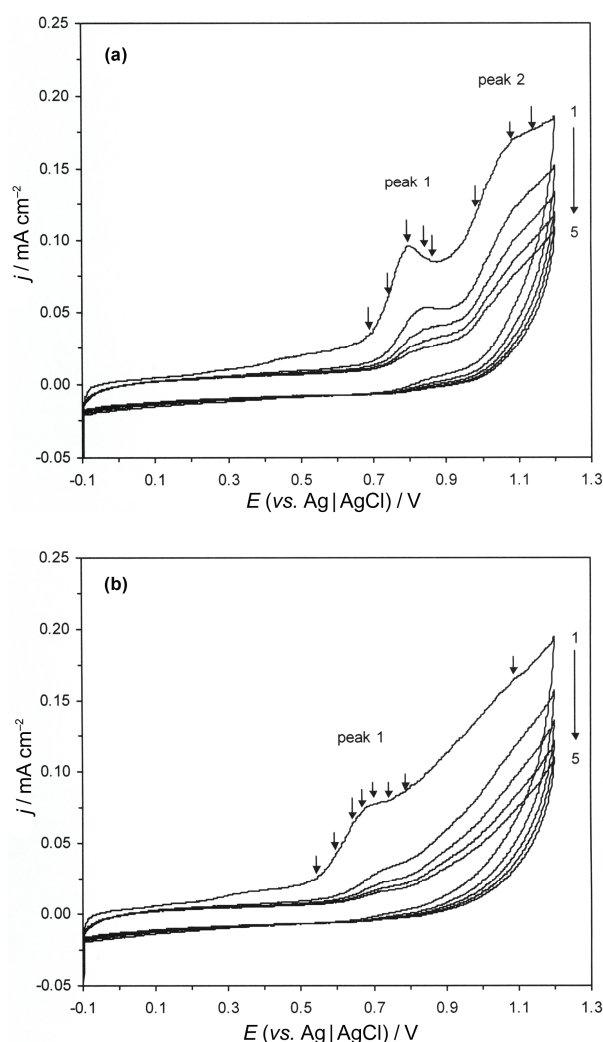


Figure 1. Cyclic voltammograms for glassy carbon electrode in 0.1 M sodium acetate – acetic acid buffer solution (in 90 % methanol), in the presence of 0.25×10^{-3} M Q 3,4'-diglc, at pH = 5.0 (a), and pH = 7.5 (b). The numbers 1 through 5 shown within the graphs correspond to the order of the recorded scans. The arrows on the first run indicate the potentials for which the impedance spectroscopy measurements were performed.

Impedance Characterization of the Process of Q 3,4'-diglc Electrooxidation at GC Electrode

Behaviour at pH = 5.0

In the present work, impedance experiments were performed in order to evaluate the process of electrooxidation of Q 3,4'-diglc molecule at the GC electrode, in contact with acetate buffer/ alcohol electrolyte, in relation to similar electrochemical works, previously published *e.g.* in Refs. 7–9, 12 and 21.

The impedance behaviour of Q 3,4'-diglc oxidation reaction at the GC electrode, in 0.1 M sodium acetate–acetic acid buffer in 90% CH₃OH solution, is shown in Figure 3, over the frequency range 1×10^5 to *ca.* 0.050 Hz. Here, at potentials close to that of the capacitive peak observed over the potential range *ca.* 0.70–0.90 V *vs.* Ag|AgCl in Figure 1a (700, 800 and 870 mV), the impedance spectra exhibit a single, distorted partial semicircle (see also the observed maxima in impedance Bode plots in Figure 4). This partial semicircle (and the corresponding charge-transfer resistance parameter, R_{F1} in Table 1) is associated with the Faradaic oxidation reaction at the 3'-OH group on ring B (see also Ref. 12). The R_{F1} resistance reaches its minimum value of $4.658 \Omega \text{ cm}^2$, at the potential very close to that of the peak current in Figure 1a (*ca.* 800 mV). For potentials positive to the peak-current, the R_{F1} parameter significantly increases, reaching $8.364 \Omega \text{ cm}^2$ at 870 mV.

Interestingly, the R_{F1} parameter values obtained for Q 3,4'-diglc are dramatically increased (by *ca.* 1.500 times) with respect to those recorded for pure quercetin, in our recently published paper in Ref. 21. This spectacular change in the reaction kinetics for Q 3,4'-diglc is a result of the catechol dihydroxyl group destabilization (as compared to the same effect on unmodified quercetin). However, significantly reduced reactivity of the 3'-OH group may partly be a consequence of a steric effect that is introduced by the presence of the glucopyranoside functional group in the 4' position on ring B.

The remaining Faradaic oxidation reaction (see peak 2 in Figure 1a) is concerned with the process of electrooxidation of the 5,7-dihydroxyl group in ring A (see also the proposed reaction mechanism in Scheme 2). Again, the R_{F2} resistance parameter reaches its minimum value of $3.678 \Omega \text{ cm}^2$ at the potential of 1.150 mV *vs.* Ag|AgCl (see again Table 1 and peak 2 in Figure 1a). Please, note that values of the R_{F2} parameter reported in this paper are in good agreement with those previously recorded for quercetin in Ref. 21.

A capacitance dispersion effect (represented by distorted semicircles) can be observed in all Nyquist plots, reported in Figure 3. Thus, a CPE-modified (constant phase element) equivalent circuit model (see the equivalent circuit in Figure 5) was used to represent the electrochemical behaviour of Q 3,4'-diglc throughout

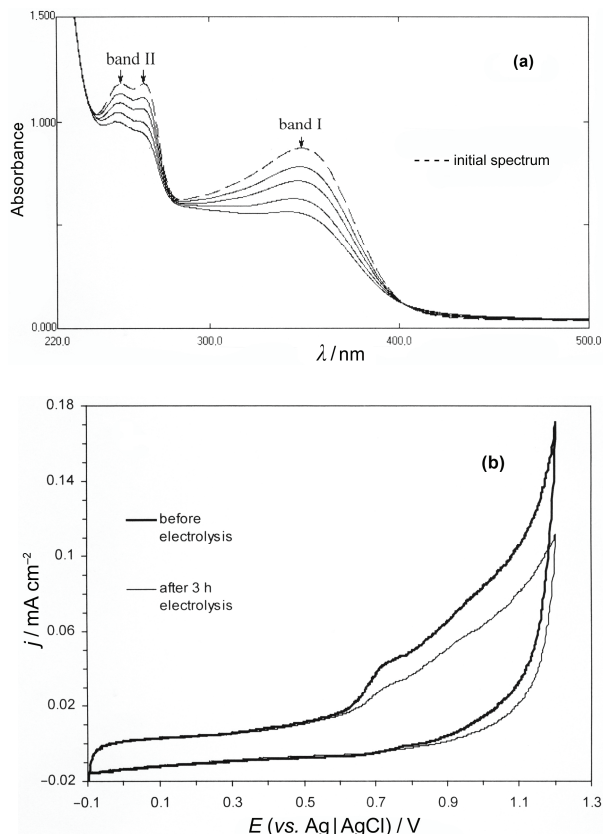


Figure 2. (a) UV-visible absorption spectra of Q 3,4'-diglc molecule at glassy carbon electrode surface, obtained during potentiostatic electrolysis carried out at 1.000 mV *vs.* Ag|AgCl, in 0.05 mM Q 3,4'-diglc, at pH = 7.5. Spectral tracing was repeated at: 30, 60, 120 and 180 minutes following electrolysis initiation. (b) CV profiles recorded during Q 3,4'-diglc electrolysis (other details as in Figure 2a).

this work. The above is likely due to increasing surface inhomogeneity^{22,23} for the GC electrode, being a result of extended potentiostatic impedance measurement (also see the values of dimensionless parameter ϕ in Table 1). The double-layer capacitance parameter (Table 1) shows small, but progressive increase from the value of $68 \mu\text{F cm}^{-2} \text{ s}^{\phi-1}$ (determined at 700 mV) to $81 \mu\text{F cm}^{-2} \text{ s}^{\phi-1}$ at 1.150 mV. Thus, a surface roughness of *ca.* 3.4 to 4.1 for the GC electrode can be assumed, when compared to a commonly used C_{dl} value in literature for smooth and homogeneous surfaces.^{24,25} In addition, for potentials negative to the capacitive peak 1 in Figure 1a (200–650 mV), the impedance behaviour was purely capacitive (with some CPE behaviour observed).

Behaviour at pH = 7.5

The impedance behaviour at pH = 7.5 is very similar to that reported for pH = 5.0. Thus, the reaction resistance R_{F1} attains its minimum value of $6.937 \Omega \text{ cm}^2$ at 680 mV, which fits very well with the position of the peak-current (peak 1 in Figure 1b). However, it is worth

Table 1. Resistance and capacitance parameters for the process of Q 3,4'-diglc reactivity at GC electrode, obtained by finding the equivalent circuit which best fitted the impedance data, as shown in Figure 5. The electrolyte was 0.1 M sodium acetate – acetic acid buffer solution in 90 % CH₃OH (at pH=5.0) and the concentration of Q 3,4'-diglc was $0.25 \times 10^{-3} \text{ mol dm}^{-3}$

E/mV	$R_{F1}/\Omega \text{ cm}^2$	$\frac{10^6 C_{dl}}{F \text{ cm}^{-2} \text{ s}^{\phi-1}}$	ϕ
700	$11,835 \pm 257$	67.6 ± 0.7	0.836 ± 0.002
750	$5,541 \pm 99$	72.1 ± 0.8	0.838 ± 0.003
800	$4,658 \pm 160$	72.4 ± 2.0	0.852 ± 0.005
840	$5,990 \pm 238$	71.3 ± 1.6	0.845 ± 0.004
870	$8,364 \pm 353$	78.2 ± 1.9	0.842 ± 0.004
	$R_{F2}/\Omega \text{ cm}^2$		
1000	$5,569 \pm 195$	79.1 ± 2.1	0.846 ± 0.005
1100	$4,357 \pm 124$	83.3 ± 1.6	0.856 ± 0.004
1150	$3,678 \pm 97$	81.0 ± 1.9	0.864 ± 0.004

Table 2. Resistance and capacitance parameters for the process of Q 3,4'-diglc reactivity at GC electrode, obtained by finding the equivalent circuit which best fitted the impedance data, as shown in Figure 5. The electrolyte was 0.1 M sodium acetate – acetic acid buffer solution in 90 % CH₃OH (at pH=7.5) and the concentration of Q 3,4'-diglc was $0.25 \times 10^{-3} \text{ mol dm}^{-3}$

E/mV	$R_{F1}/\Omega \text{ cm}^2$	$\frac{10^6 C_{dl}}{F \text{ cm}^{-2} \text{ s}^{\phi-1}}$	ϕ
550	$16,395 \pm 636$	41.1 ± 1.1	0.863 ± 0.005
600	$7,932 \pm 216$	51.3 ± 1.0	0.874 ± 0.003
650	$7,011 \pm 249$	40.6 ± 1.2	0.890 ± 0.005
680	$6,937 \pm 219$	43.0 ± 1.0	0.862 ± 0.004
700	$8,350 \pm 250$	46.9 ± 0.8	0.867 ± 0.003
750	$8,714 \pm 362$	43.1 ± 1.4	0.875 ± 0.005
	$R_{F2}/\Omega \text{ cm}^2$		
800	$7,374 \pm 355$	53.4 ± 1.6	0.880 ± 0.005
1100	$3,060 \pm 117$	56.1 ± 1.9	0.884 ± 0.005

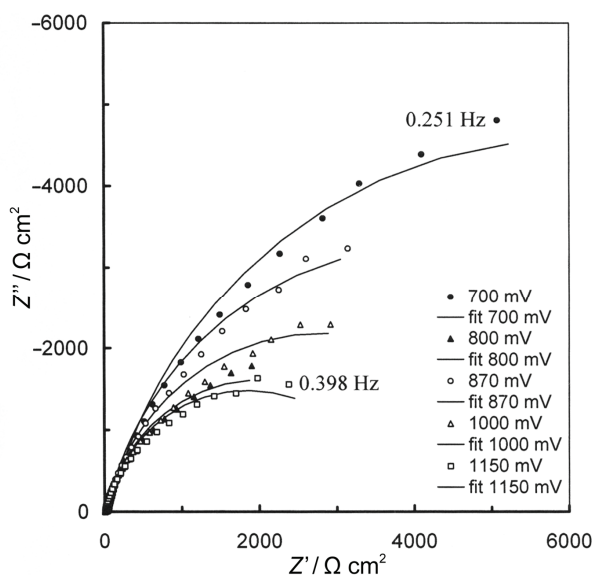


Figure 3. Complex-plane impedance plots for the process of electrooxidation of Q 3,4'-diglc on GC electrode, in contact with 0.1 M sodium acetate – acetic acid buffer in 90 % CH₃OH solution, recorded at 293 K for the five stated potential values. The solid lines correspond to representation of the data according to the equivalent circuit shown in Figure 5.

mentioning that the voltammetric profiles for peak 1 in Figure 1b are appreciably shifted (by *ca.* 150 mV) towards less positive potentials, as compared to those recorded in acidic solution in Figure 1a. Thus, partial deprotonation of the molecule (much more extensive at neutral pH than in acidic solution¹⁸) results in significant enhancement of the electron-transfer process.

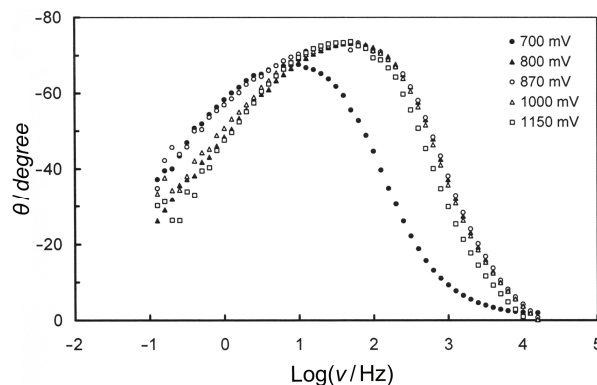


Figure 4. Bode phase-angle plots for the process of electrooxidation of Q 3,4'-diglc on GC electrode, for the stated potential values (other details as in Figure 3).

Although the recorded values of the R_{F1} resistance parameter in Table 2 are significantly higher than those derived from acidic solution in Table 1, it has to be noted that the electrochemically active surface area in neutral solution is significantly smaller than that available in acidic electrolyte. Thus, in contrast to the behaviour at pH = 5.0, the double-layer capacitance values at pH = 7.5 are significantly smaller and oscillate between 41 and $56 \mu\text{F cm}^{-2} \text{ s}^{\phi-1}$.

The behaviour of the R_{F2} parameter in Table 2 follows that already reported for peak 2 in Table 1. In addition, no considerable shift of the voltammetric profiles for peak 2 (compare Figure 1a with Figure 1b) was observed. This is because the stabilization effect for a dihydroxyl moiety in the *meta* position (ring A) is much weaker than that in the *ortho* position (ring B).

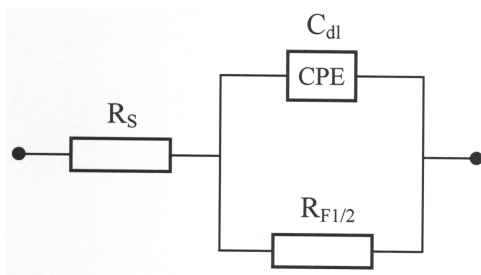


Figure 5. Equivalent circuit for the process of electrooxidation of Q 3,4'-diglc at GC electrode. The circuit exhibits a Faradaic charge-transfer resistance, R_{F1} (R_{F2}), which parameter is in a parallel combination with the double-layer capacitance, C_{dl} (represented as the CPE element for distributed capacitance), jointly in series with an uncompensated solution resistance, R_S .

CONCLUSIONS

Electrooxidation behaviour of Q 3,4'-diglc molecule at glassy carbon electrode surface was examined by means of a.c. impedance spectroscopy, linear-sweep voltammetry and UV-visible spectroscopy techniques.

A two-step surface electrooxidation process (as evidenced by the UV-visible spectral analysis) commences at the 3'-OH group on ring B, which is then followed by oxidation of the 5,7-dihydroxyl group of ring A. The initial oxidation step (involving the 3'-OH group) showed significant pH-dependence. Thus, facilitated deprotonation of the 3'-OH group at neutral pH resulted in considerable enhancement of the charge-transfer process. Moreover, the presence of the glucopyranoside functional group at the 4' position of ring B led to spectacular increase of the reaction resistance parameter (by *ca.* 1.500 times at pH = 5.0), as compared to that recently recorded for unmodified quercetin. Hence, it is evident that there is a strict and important relationship between a molecular structure of a flavonoid and its oxidation properties.

REFERENCES

1. L. Pourcel, J. M. Routaboul, V. Cheynier, L. Lepiniec, I. Debeaujon, *Trends Plant Sci.* **12** (2006) 29.
2. W. Wiczowski, J. Romaszko, A. Bucinski, D. Szawara-Nowak, J. Honke, H. Zielinski, M. K. Piskula, *J. Nutr.* **138** (2008) 885.
3. B. Yang, A. Kotani, K. Arai, F. Kusu, *Anal. Sci.* **17** (2001) 599.
4. M. M. Silva, M. R. Santos, G. Caroco, R. Roha, G. Justino, L. Mira, *Free Rad. Res.* **36** (2002) 1219.
5. D. Tsimogiannis and V. Oreopoulou, *J. Amer. Oil Chem. Soc.* **84** (2007) 129.
6. Y. H. Son, W. K. Jung, Y. J. Jeon, S. K. Kim, C. H. Lee, *Eur. Food Res. Technol.* **226** (2008) 473.
7. H. P. Hendrickson, A. D. Kaufman, C. E. Lunte, *J. Pharm. Biomed. Anal.* **12** (1994) 325.
8. A. K. Timbola, C. D. Souza, C. Soldi, M. G. Pizzolatti, A. Spinelli, *J. Appl. Electrochem.* **37** (2007) 617.
9. A. Zhou, S. Kikandi, O. A. Sadik, *Electrochem. Commun.* **9** (2007) 2246.
10. H. R. Zare, M. Namazian, N. Nasirizadeh, *J. Electroanal. Chem.* **584** (2005) 77.
11. S. Martinez, L. Valek, Z. Petrović, M. Metikoš-Huković, I. Piljac, *J. Electroanal. Chem.* **584** (2005) 92.
12. P. Janeiro and A. M. O. Brett, *Anal. Chim. Acta* **518** (2004) 109.
13. D. Zielinska, L. J. Nagels, M. K. Piskula, *Anal. Chim. Acta* **617** (2008) 22.
14. A. Wach, K. Pyrzynska, M. Biesiaga, *Food Chem.* **100** (2007) 699.
15. A. Adrian, A. A. Franke, L. J. Custer, C. Arakaki, S. P. Murphy, *J. Food Compos. Anal.* **17** (2004) 1.
16. J. R. Macdonald, *Electrochim. Acta* **35** (1990) 1483.
17. M. E. Ghica and A. M. O. Brett, *Electroanalysis* **17** (2005) 313.
18. K. Lemanska, H. Szymusiak, B. Tyrakowska, R. Zielinski, A. E. M. F. Soffers, I. M. C. M. Rietjens, *Free Rad. Biol. Med.* **31** (2001) 869.
19. V. Castaignede, H. Durliat, M. Comtat, *Anal. Lett.* **36** (2003) 1707.
20. J. B. He, Y. Wang, N. Deng, X. Q. Lin, *Bioelectrochem.* **71** (2007) 157.
21. D. Zielinska and B. Pierozynski, *J. Electroanal. Chem.* **625** (2009) 149.
22. T. Pajkossy, *J. Electroanal. Chem.* **364** (1994) 111.
23. B. E. Conway, in: E. Barsoukov, J. Ross Macdonald (Eds.), *Impedance Spectroscopy. Theory Experiment and Applications*, Wiley-Interscience, John Wiley & Sons Inc., Hoboken, NJ, 2005, p. 494, (Chapter 4.5.3.8)
24. A. Lasia and A. Rami, *J. Applied Electrochem.* **22** (1992) 376.
25. L. Chen and A. Lasia, *J. Electrochem. Soc.* **138** (1991) 3321.

SAŽETAK

Proces elektrooksidacije 3,4'-di-*O*- β -glukopiranozida kvercetina na elektrodi od staklastog ugljika

Boguslaw Pierozynski i Danuta Zielinska

*Department of Chemistry, Faculty of Environmental Management and Agriculture,
University of Warmia and Mazury in Olsztyn, Plac Lodzki 4, 10-727 Olsztyn, Poland*

Elektrokemijskim i spektroskopskim (UV-VIS) metodama ispitan je proces elektrooksidacije molekule 3,4'-di-*O*- β -glukopiranozida kvercetina (Q 3,4'-diglc) na elektrodi od staklastog ugljika u 0.1 M otopini acetatnog pufera koja sadrži 90 % metanola. Prvo se oksidira skupina 3'-OH (u prstenu B), nakon toga oksidaciji podliježu hidrok-silne skupine u položaju 5,7-di-OH (u prstenu A). Površina elektrode je snažno blokirana produktima oksidacije Q 3,4'-diglc.